Single Molecule Imaging of Transcription Factor Binding to DNA in Live Mammalian Cells

Supplementary Information

J Christof M Gebhardt[1,6], David M Suter[1,6], Rahul Roy[1,4], Ziqing W Zhao[1,2], Alec R Chapman[1,2], Srinjan Basu[1,3,5], Tom Maniatis[3], and X Sunney Xie[1]

[1]Department of Chemistry and Chemical Biology, Harvard University, Cambridge, Massachusetts, USA

[2]Graduate Program in Biophysics, Harvard University, Cambridge, Massachusetts, USA

[3]Department of Biochemistry and Molecular Biophysics, Columbia University Medical Center, New York, New York, USA

[4]Current address: Department of Chemical Engineering, Indian Institute of Science, Bangalore, India

[5]Current address: Department of Biochemistry, University of Cambridge, Cambridge, United Kingdom

[6]These authors contributed equally to this work

Correspondence should be addressed to X.S.X (xie@chemistry.harvard.edu)

Supplementary Figure 1

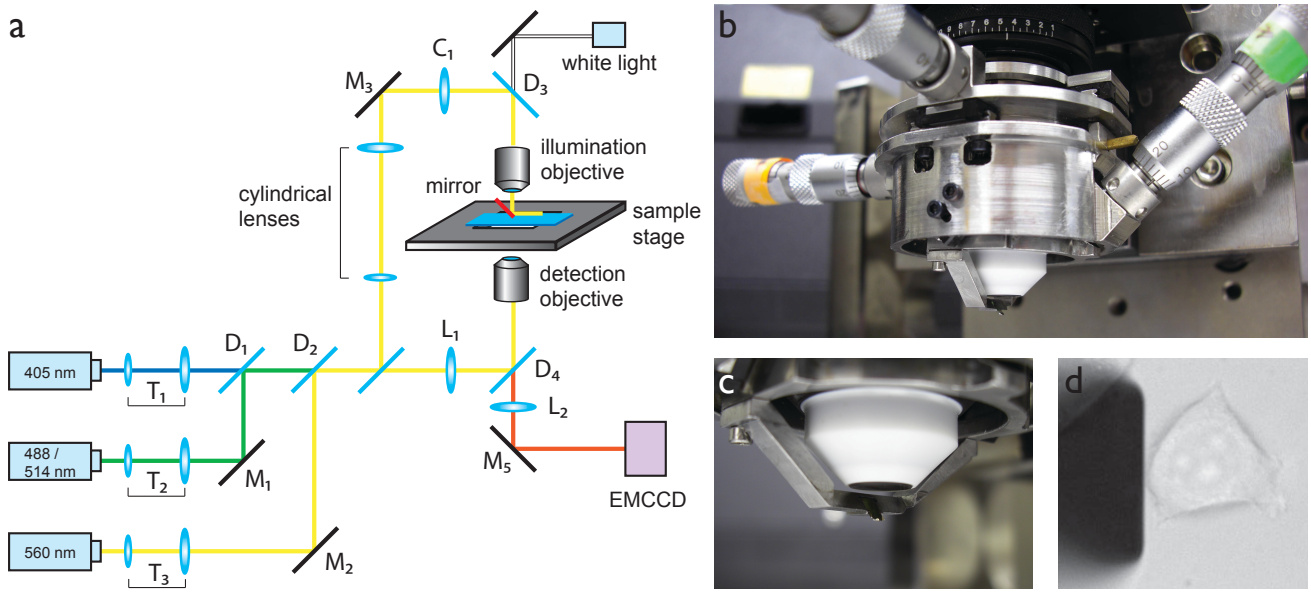

Setup of the reflected light sheet microscope. (**a**) Scheme of the setup. Lasers are collimated (telescope T_1 – T_3) and aligned (mirrors M_1 and M_2 and dichroic beamsplitters D_1 and D_2). A cylindrical lens telescope and cylindrical lens C_1 create an expanded and collimated line that overfills the back aperture of the illumination objective. After the illumination objective, laser beams are reflected off an AFM cantilever and focused to a diffraction limited sheet. Alternatively, laser beams are focused by L_1 and reflected by dichroic D_4 for wide field illumination. Fluorescent light is collected by the imaging objective and focused by L_2 onto an electron-multiplying CCD (EMCCD) chip. (**b**) Photograph of the illumination objective. A home built xyz-device is clamped to the objective and holds the AFM cantilever. (**c**) Close up of the illumination objective and the metal device that holds the AFM cantilever. (**d**) bright field image (as seen on the EMCCD) of the AFM cantilever (left) positioned next to a MCF-7 cell (right).

Supplementary Figure 2

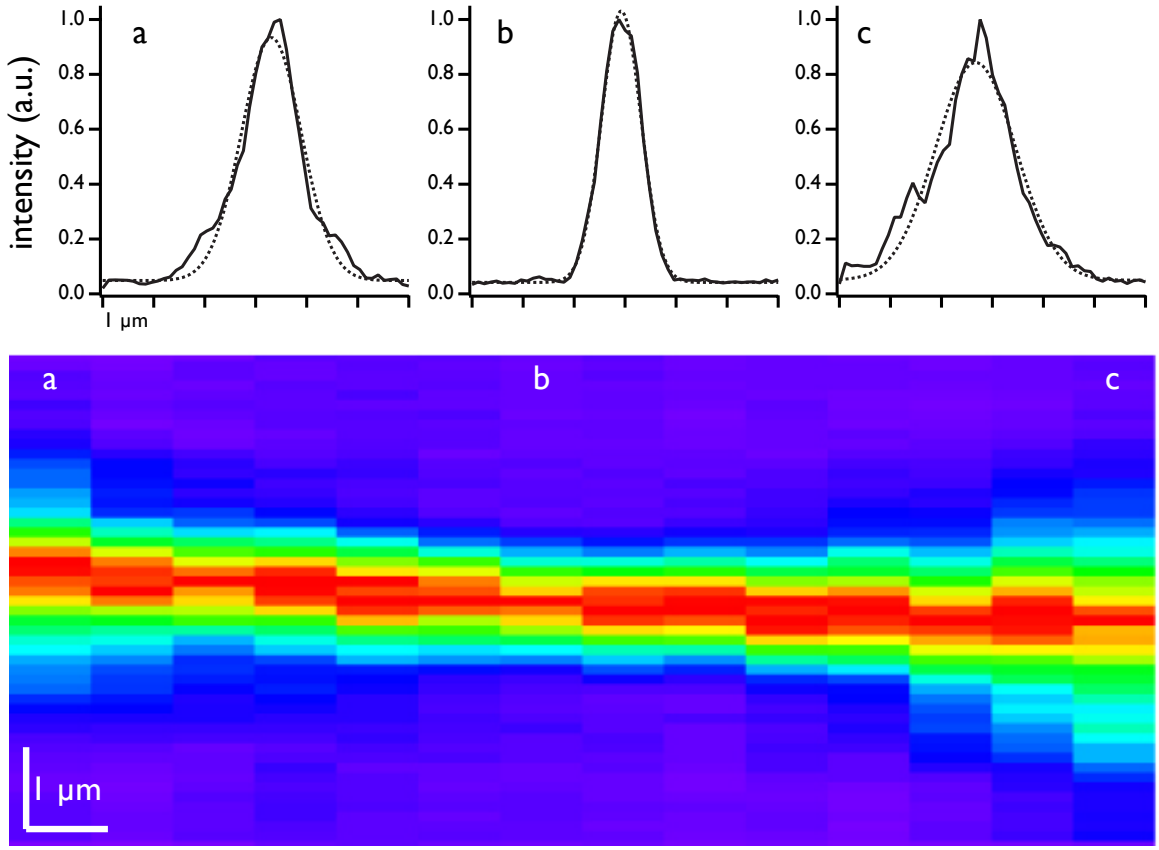

Intensity profile of the light sheet after reflection. Shown is the intensity of a fluorescent bead scanned vertically through the light sheet at 4 mm aperture size after reflection by the AFM cantilever (lower panel). (**a**) – (**c**) Intensity profiles of the bead at the indicated positions (continuous line) and Gaussian fit (dashed line). Data is from the same data set as Figure 1b in the main text. The light sheet displays a small deviation from the horizontal plane (2°), which corresponds to a 2% deviation from the 45° cantilever angle.

Supplementary Figure 3

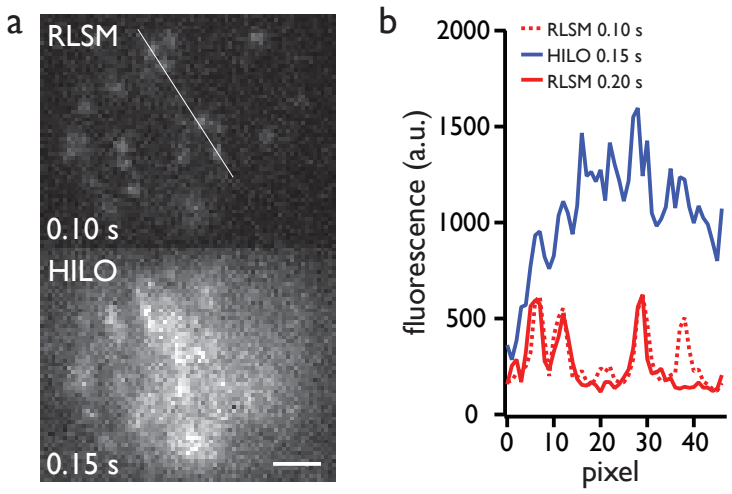

Comparison between RLSM and HILO at high density of fluorescent proteins. (**a**) MCF-7 cell expressing mEos2-H4 molecules, alternately imaged with RLSM and HILO after high activation of mEos2 with 405 nm laser. Scale bar, 2 μm. (**b**) Fluorescence intensity along the white line for RLSM at 0.10 s (dotted red line) and 0.20 s (red line) and HILO at 0.15 s (blue line). The three single molecules detected in both RLSM images should also appear in the HILO image, since it was recorded in the intervening period. However, due to the large and inhomogeneous background in the HILO image, the assignment of single molecules is ambiguous.

Supplementary Figure 4

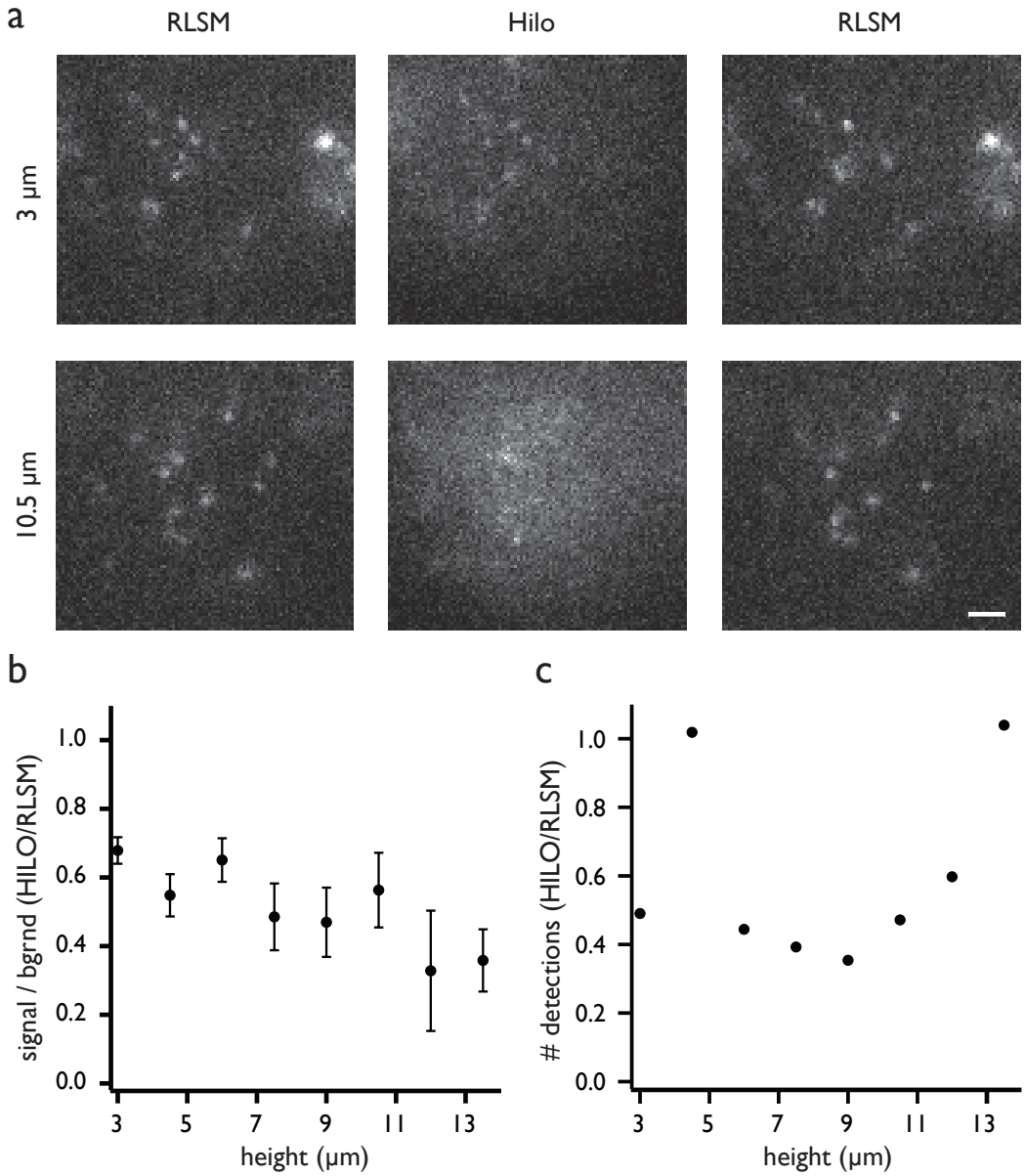

Comparison between RLSM and HILO at different z-positions. (**a**) Successive images of a MCF-7 cell expressing mEos2-H4 molecules, alternately imaged with RLSM and HILO at different z-sections with 50 ms integration time. Scale bar is 2 µm. (**b**) Ratio of HILO SBR and RLSM SBR of single molecules at different z-sections (n = 8 cells, error bars represent ± s.e.m.). (**c**) Ratio of the number of molecules detected with HILO and RLSM at different z-sections for the cell shown in (a).

Supplementary Figure 5

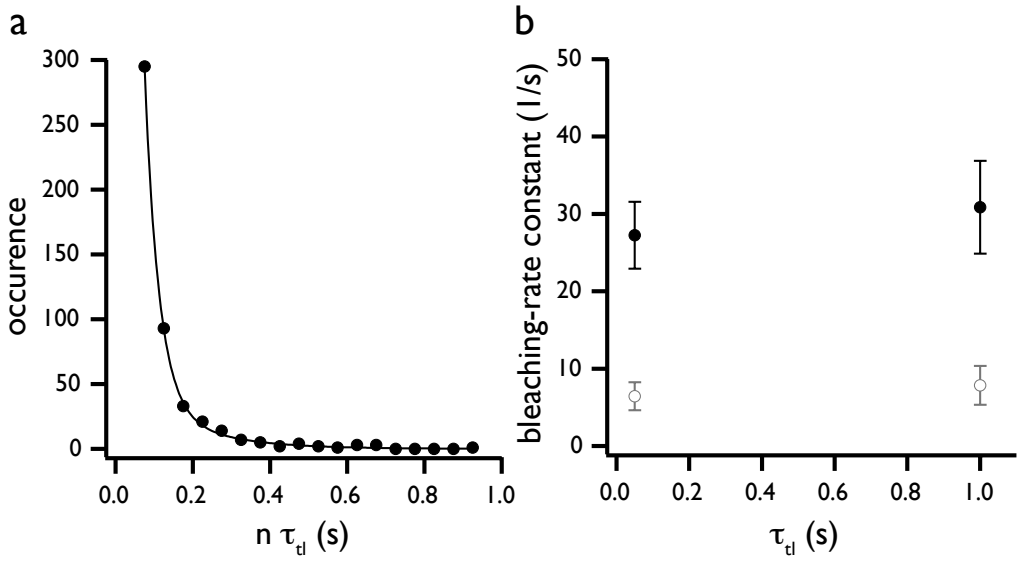

In vitro characterization of YPet photobleaching. YPet protein fused to a His-tag was expressed in E.Coli, purified with a Ni-NTA column, unspecifically adsorbed to the surface and washed with OptiMEM medium. The reflecting mirror was removed and the focal line of the vertical light sheet was used for excitation, to achieve an illumination intensity comparable to *in vivo* experiments. (**a**) Frequency histogram of YPet 'on' times at continuous illumination with 50ms frame acquisition rate (time-lapse duration τ_{tl} = 0.05 s). The distribution is best fit with a two-exponential decay function yielding two different photobleaching rate constants. (**b**) Photobleaching rate constants obtained at 0.05 s (*n* = 484) and 1 s time-lapse conditions (*n* = 412), with 50ms integration time. The dark time was ignored in the analysis to allow comparison of both rate constants. The proportion of the fast rate constant (full symbols) is in both conditions 97%. Error bars represent ± s.d.

Supplementary Figure 6

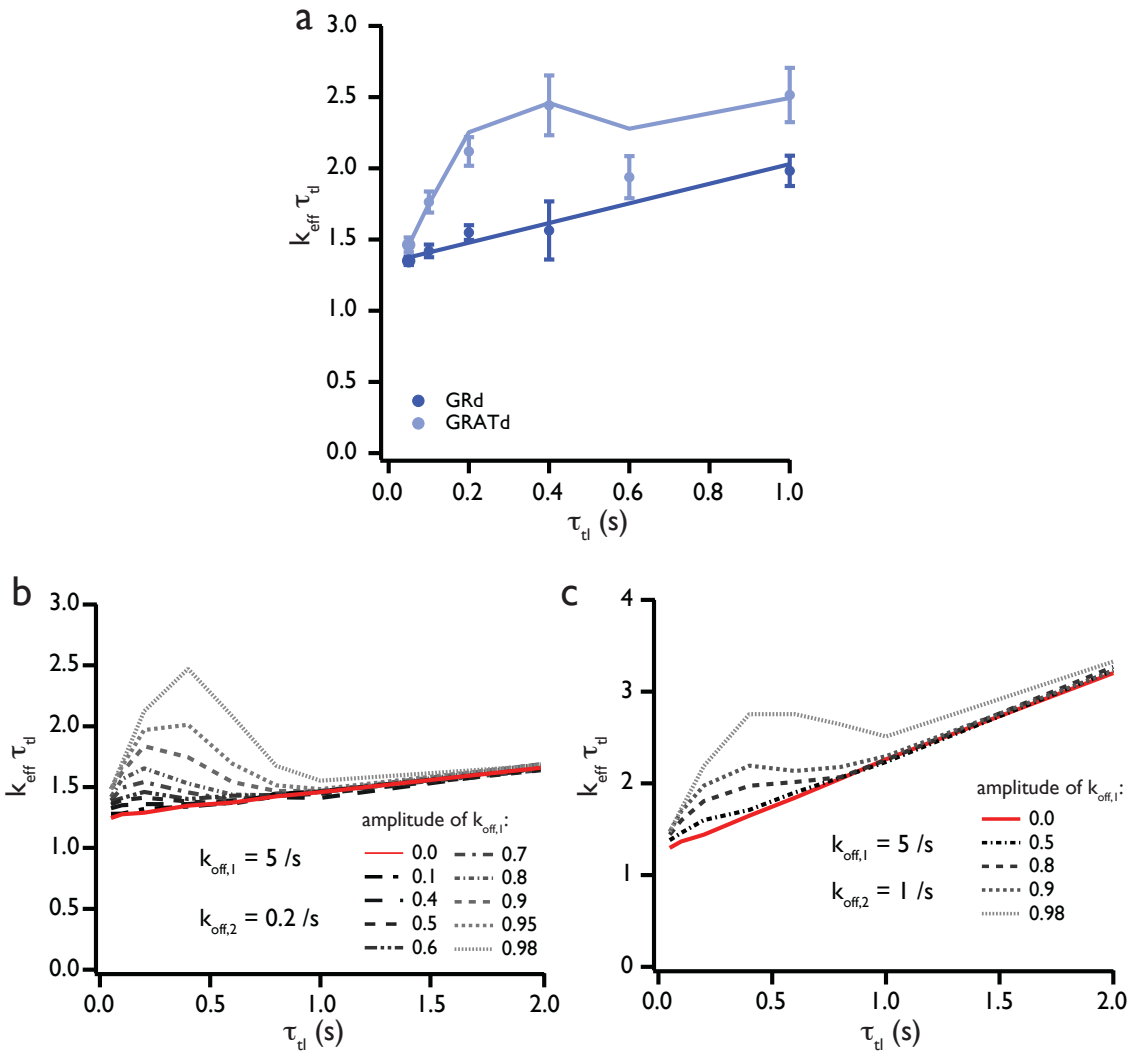

Resolution of two populations with different off-rate constants of monomeric GR. (**a**) Effective rate constant (exponent from a single exponential fit to a histogram of residence times at a given time-lapse duration) as function of time-lapse duration for GR A458T (induced with 100 nM dexamethasone, light blue, *n* = 1274 (0.05 s), *n* = 846 (0.1 s), *n* = 681 (0.2 s), *n* = 253 (0.4 s), *n* = 260 (0.6 s), *n* = 277 (1.0 s), 29 cells). The data of induced GR (dark blue) is shown for comparison (see **Fig. 2b**). Values of effective rate constants for induced GR were fit with a straight line. For GR A458T the line indicates the effective rate constants obtained from single exponential fits to residence time histograms simulated with two off-rate constants (values and fractions of both off-rates for the Monte-Carlo simulation were obtained from a global fit with a sum of two exponential functions to the measured residence time histograms). Error bars represent ± s.d. (**b**) and (**c**) Residence time histograms for each time-lapse duration were simulated with two off-rate constants and varying amplitude of the fast off-rate. The effective rate constant was obtained as the exponent from single exponential fits to the histograms. In both cases a second fast rate constant can only be resolved if its amplitude is > 0.5.

Supplementary Figure 7

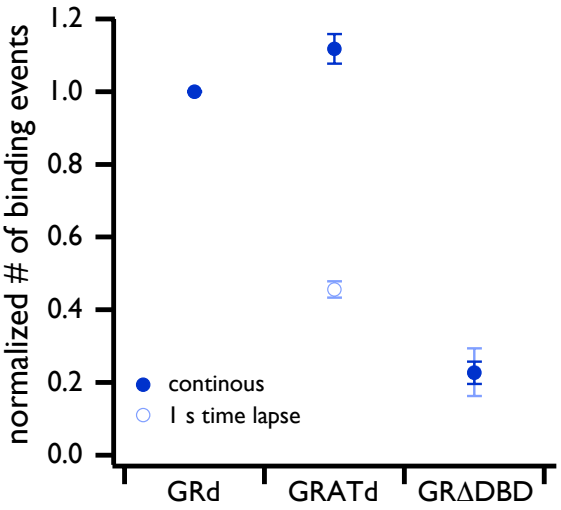

Comparison of the number of binding events between GR, GR A458T and GR ΔDBD (all induced with 100 nM dexamethasone), normalized with respect to video duration, nuclear area and average intensity of the nucleus. The value of GR is set to 1. Error bars represent ± s.e.m. (GR: *n* = 8 cells (continous), *n* = 8 cells (1.0 s); GR A458T: *n* = 9 cells (continous), *n* = 12 cells (1.0 s); GR ΔDBD: *n* = 6 cells (continous), *n* = 8 cells (1.0 s)).
The number of binding events observed in the 1.0 s time-lapse condition for GR A458T is smaller than for GR, consistent with a majority of GR A458T molecules exhibiting a fast dissociation rate constant compared to GR (only molecules bound for 2 frame are counted as bound molecules). For GR ΔDBD, few bound molecules are observed in both time-lapse conditions.

Supplementary Figure 8

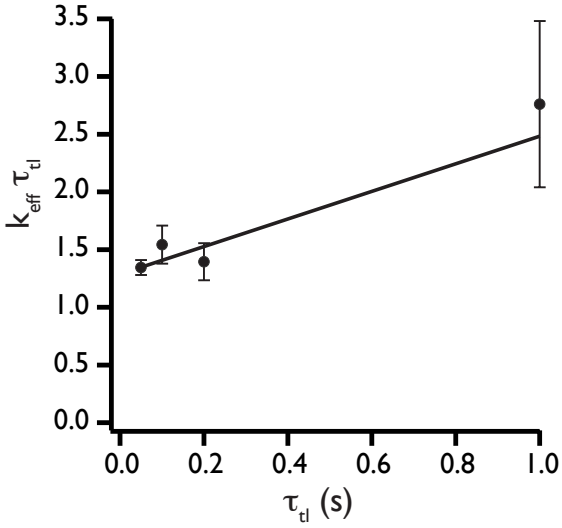

Effective rate constant as function of time-lapse duration for GR ΔDBD in MCF-7 cells induced with 100nM dexamethasone. Error bars represent ± s.d. (*n* = 584 (0.05 s), *n* = 135 (0.1 s), *n* = 109 (0.2 s), *n* = 35 (1.0 s), 16 cells).

Supplementary Figure 9

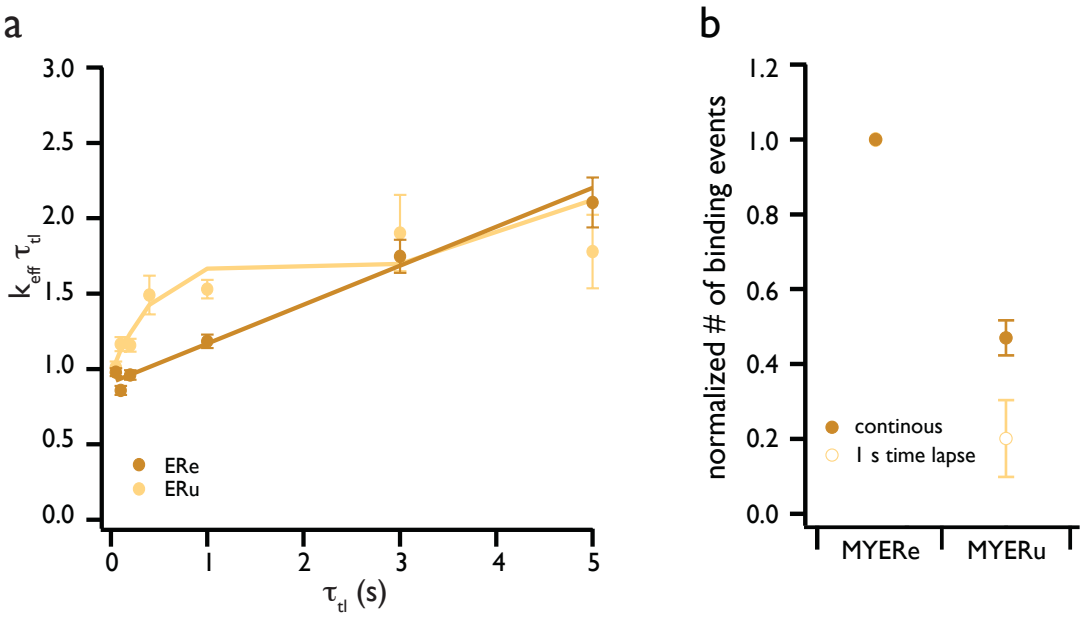

DNA binding properties of ER. (**a**) Effective rate constant (exponent from a single exponential fit to a histogram of residence times at a given time-lapse duration) as function of time-lapse duration for ER (induced with 100 nM β-estradiol, dark yellow) and uninduced ER (light yellow). Values of effective rate constants for induced ER were fit with a straight line. For uninduced ER the line indicates the effective rate constants obtained from single exponential fits to residence time histograms simulated with two off-rate constants (values and fractions of both off-rates for the Monte-Carlo simulation were obtained from a global fit with a sum of two exponential functions to the measured residence time histograms). Error bars represent ± s.d. (induced ER: *n* = 1848 (0.05 s), *n* = 1072 (0.1 s), *n* = 1254 (0.2 s), *n* = 927 (1.0 s), *n* = 393 (3.0 s), *n* = 281 (5.0 s), 7 cells; uninduced ER: *n* = 1089 (0.05 s), *n* = 813 (0.1 s), *n* = 983 (0.2 s), *n* = 214 (0.4 s), *n* = 876 (1.0 s), *n* = 109 (3.0 s), *n* = 80 (5.0 s), 14 cells) (**b**) Comparison of binding events of ER (induced with 100 nM β-estradiol) and uninduced ER, normalized with respect to movie duration, nuclear area and average intensity of the nucleus. The value of ER is set to 1. Error bars represent ± s.e.m. (induced ER: *n* = 5 cells (continous), *n* = 5 cells (1.0 s); uninduced ER: *n* = 7 cells (continous), *n* = 4 cells (1.0 s)).

Supplementary Figure 10

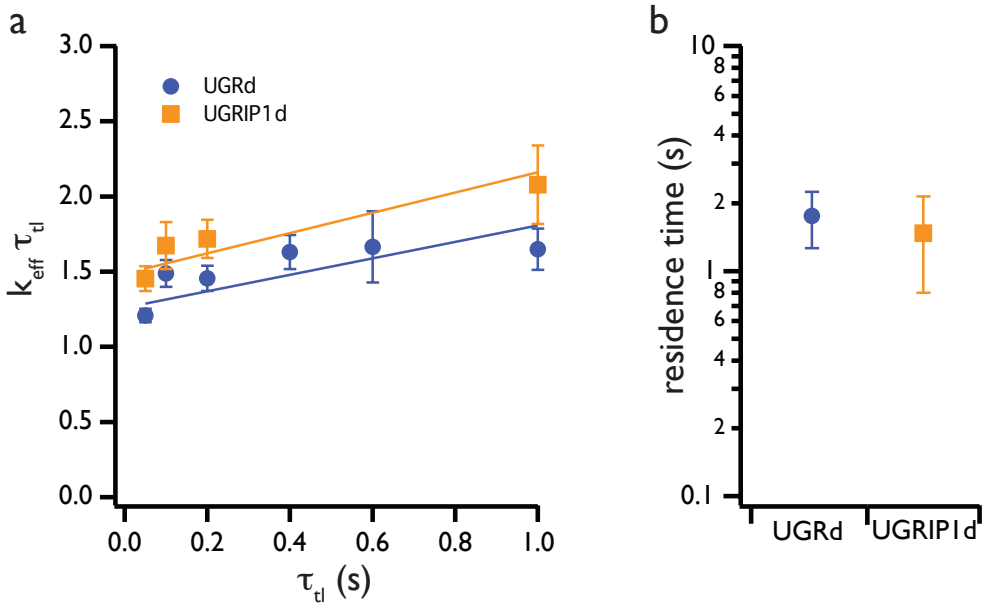

DNA binding properties of GR and GRIP1 in U2-OS cells. (**a**) Effective rate constant as function of time-lapse duration for glucocorticoid receptor (UGRd) and glucocorticoid receptor interacting protein 1 (UGRIP1d) in the presence of 100 nM dexamethasone in U2-OS cells. Error bars represent ± s.d. (UGRd: *n* = 987 (0.05 s), *n* = 441 (0.1 s), *n* = 442 (0.2 s), *n* = 306 (0.4 s), *n* = 81 (0.6 s), *n* = 202 (1.0 s), 26 cells; UGRIP1d: *n* = 445 (0.05 s), *n* = 196 (0.1 s), *n* = 273 (0.2 s), *n* = 110 (1.0 s), 10 cells) (**b**) Residence times of GR and GRIP1. Error bars represent ± s.d. (see online methods).

Supplementary Table 1

YPet-protein fusion	$t_{res,1}$ (s)	$t_{res,2}$ (s)	% $t_{res,1}$
MCF-7 GRd	1.45 ± 0.25		
MCF-7 GR A458Td	0.15 ± 0.02	0.76 ± 0.12	97 ± 2
MCF-7 GR ΔDBDd	0.76 ± 0.35		
U2-OS GRd	1.75 ± 0.49		
U2-OS GRIP1d	1.47 ± 0.67		
MCF-7 ERe	3.85 ± 0.30		
MCF-7 ERu	0.65 ± 0.14	4.35 ± 0.95	87 ± 5

Residence times of various transcription factors measured in MCF-7 or U2-OS cells stably expressing the fusion protein. Values were obtained as described in online methods. GRd: glucocorticoid receptor, GR A458Td: mutant A458T of GR, GR ΔDBDd: GR mutant without DNA binding domain, GRIP1: glucocorticoid receptor interacting protein 1, d indicates induction with 100 nM dexamethasone; ER: estrogen receptor, e: induced with 100 nM β-estradiol, u: uninduced. Errors represent ± s.d.

Supplementary Table 2

Primer names	Primer sequences
Ypet_forward	CCGAATTCATGGTGAGCAAAGGCGAA
Ypet_reverse	CCTCTAGACTTATAGAGCTCGTTCATGCCC
eGFP_forward	AAGAATTCACCATGGTGAGCAAGGGCGAG
eGFP_reverse	AATCTAGACTTGTACAGCTCGTCCATGC
TagRFP_forward	CCGAATTCATGGTGTCTAAGGGCGAAGA
TagRFP_reverse	GGTCTAGACTTGTACAGCTCGTCCATGC
GR_forward	CCTCTAGAATGGACTCCAAAGAATCATTAACTC
GR_reverse	AAGGCGCGCCTCACTTTTGATGAAACAGAAGTTTTT
GR for mEos2fusion_forward	AAACTCGAGGTTAATATGGACTCCAAAGAATC
GR for mEos2fusion_reverse	TGCGGCCGCTCATTATCACTTTTGATGAAACAGAAG
GRA458T_forward	TGGAAGGACAGCACAATTACCTATGTACCGGAAGGAATGATTG
GRA458T_reverse	CAATCATTCCTTCCGGTACATAGGTAATTGTGCTGTCCTTCCA
GRΔDBD5'_forward	AAGGATCCATGGACTCCAAAGAATCATTAACTC
GRΔDBD5'_reverse	AAACCGGTGAGTTTGGGAGGTGGTCCT
GRΔDBD3'_forward	AAACCGGTAACCTGGAAGCTCGAAAAACA
GRΔDBD3'_reverse	GGTTAATTAATCACTTTTGATGAAACAGAAGTTTTT
ER_forward	GAACTAGTATGACCATGACCCTCCACA
ER_reverse	AAGGCGCGCCTCAGACCGTGGCAGGG
GRIP-1_forward	CCTCTAGAATGAGTGGGATGGGAGAAAAT
GRIP-1_reverse	AAGGCGCGCCTCAGCAATATTTCCGTGTTGTG
H4_forward	AAACTCGAGGTTAATATGTCAGGACGCGGC
H4_reverse	TGCGGCCGCTCATTATTAGCCGCCGAAGCC
Bmal1_forward	AATCTAGAATGGCGGACCAGAGAATG
Bmal1_reverse	AAGGCGCGCCCTACAGCGGCCATGGC
Clock_forward	AAACTAGTATGGTGTTTACCGTAAGCTGTAGTAA
Clock_reverse	AAGGCGCGCCCTACTGTGGCTGGACCTTGGA

Primers used for protein fusion constructs.